NUMERICAL INVESTIGATION OF THE FLOW AROUND A CYLINDER FOR THE FORECASTING OF VORTICES

Jean Stéphane Armougom, armougom.stephane@gmail.com
Arts et Metiers Paristech - 147, boulevard de l'Hôpital 75013 Paris, France.
Budapest University of Technology and Economics - Műegyetem rkp. 3-9. H-1111 Budapest, Hungary.

Julianna Vulcão da Silva, juliannavs@yahoo.com.br
Hamilton Pessoa Picanço, hamilton_picanco@yahoo.com.br
Naval Engineering Department - Federal University of Pará - Belém, PA, 66075-110, CEP: 66075-110, Brazil.

Danielle R.S. Guerra, daguerra@ufpa.fr
Mechanical Engineering Department - Federal University of Pará - Belém, PA, 66075-110, CEP: 66075-110, Brazil.

Abstract. *Within the aim to investigate the behaviour of the flow past an electric cable a 2D numerical simulation has been carried out using the commercial code Fluent. In this research study the electric cable is modelled as a smooth fixed cylinder due to the similarity shape they share. The multi-block approach in the geometric modelling of the domain has been applied in order to achieve a structured grid matching properly the cylinder contour. The geometric domain has been discretized using a typical 2D quadrilateral element. The Shear-Stress Transport (SST) k-ω turbulence model has been used to investigate the vortex-shedding phenomenon. The drag coefficient, the lift coefficient and the vortex shedding frequency have been derived from the simulation and compared with the literature. To tackle the problem of dependency of the numerical solution regarding the grid, a convergence study has been initiated. Unfortunately due to the computational resources necessary the convergence study has not yet been completed, but the last obtained results are in accordance with literature.*

1. INTRODUCTION

The incidence of the wind on the transmission lines may involve vibrations in their structures leading, after some time of service, to their ruptures. The objective of the present work is to analyze the phenomenon of vortex shedding around a circular cylinder, modelling the conductor, within the aim to get knowledge on the alternative action of the fluid. In this first work the cylinder is modelled as a smooth fixed cylinder. A 2D numerical simulation has been carried out using the commercial code Fluent. The geometry and the grid have been performed using the associated software Gambit. The medium is the air considered as incompressible, viscous and Newtonian. The Shear-Stress Transport (SST) $k-\omega$ turbulence model has been used as it seems to be the most suitable to well-capture the essence of the relevant flow characteristics. A convergence study has been carried out to ensure the independence of the numerical solution from the grid resolution but must be finalized. Finally the last part is devoted to the comparison of the last obtained simulation results with experimental and empirical data from the literature.

The study of flow over cylinders and their behavior under the influence of the fluid on its structure is an important subject in the scientific community due to its various applications. As an example of the importance of the study considering the effects of flow on the cylindrical structure submerged by Leonard and Roshko (2001) have been analyzed the aspects of the vibration during the passage of the flow. This phenomenon in cylindrical structures is due to the formation of vortices in the wake of the cylinder, known as Vortex Induced Vibration (VIV). Indeed with respect to oscillation of the cylinder Williamson (1996) studied the dynamics of vortices with respect to new developments involving the vortex shedding in the wake of these structures. Sumer and Fredsoe (2006) have presented a hydrodynamic study around cylindrical structures with information about the flow, the forces developed due to interaction between body and fluid, the behavior when the cylinder is oscillating and the phenomenon of vortex induced vibrations when the body is in current movements to stable or irregular waves.

However, despite the simple form, the study of flow over cylinders is of great importance and involves turbulence phenomena, domain analysis, mesh and numerical models for complex solutions which consume time and study, but may provide satisfactory results for its various applications.

2. NUMERICAL INVESTIGATION

The electric cable is modelled as a circular smooth cylinder due to the obvious shape similarity they share. This part describes the 2D numerical investigation of the flow past a fixed smooth circular cylinder at $Re = 20{,}538$ using the SST $k-\omega$ turbulence model.

2.1. Mathematical model

2.1.1. Low velocity aerodynamic assumption

The low velocity aerodynamic is based on several hypotheses (Hémon, 2006) as mentioned below:

- The air is considered as a Newtonian fluid i.e. the stress tensor is linearly related to the strain tensor with the fluid viscosity as coefficient of proportionality.
- The Mach number *M*, defined by the ratio between the air velocity *U* and the sound velocity *c*, manifests the compressibility effects of the air. For Mach numbers below *0.3*, corresponding to a flow velocity below *100m/s*, the air can be considered as incompressible.
- The temperature of the air is assumed constant.
- The air is a light gas; hence its gravity force is neglected with regards to the other present forces.

2.1.2. Basic equations

The basic fluid mechanics equations rely on the Navier-Stokes equations which encompass a continuity equation and a momentum conservation equation. From the unsteady Reynolds Averaged Navier-Stokes (RANS) equations (FLUENT, 2005) and considering the low velocity aerodynamic assumptions, the RANS equations can be re-written in the Cartesian tensor as follows:

$$\frac{\partial u_i}{\partial x_i} = 0 \tag{1}$$

$$\rho \frac{\partial \mathrm{u_i}}{\partial \mathrm{t}} + \rho \mathrm{u_i} \frac{\partial \mathrm{u_i}}{\partial \mathrm{x_j}} = -\frac{\partial \mathrm{p}}{\partial \mathrm{x_i}} + \frac{\partial}{\partial \mathrm{x_j}}\left(2\mu \mathrm{S_{ij}}\right) + \frac{\partial}{\partial \mathrm{x_j}}(-\overline{\rho \mathrm{u_i' u_j'}}) \tag{2}$$

Where u is the averaged velocity, p is the averaged static pressure, μ is the dynamic viscosity, $S_{ij} = \frac{1}{2}(\frac{\partial u_i}{\partial x_j} + \frac{\partial u_j}{\partial x_i})$ is the averaged strain rate tensor and is the Reynolds stresses.

The Reynolds stresses terms represent the effects of turbulence and must be modelled for closing the Reynolds-averaged momentum equation system Eq. (2). They are modelled using the Boussinesq hypothesis (FLUENT, 2005) which is given for an incompressible flow by Eq. (3).

$$-\overline{\rho \mathrm{u_i' u_j'}} = 2\mu_t \mathrm{S_{ij}} - \frac{2}{3}\rho \mathrm{k}\delta_{\mathrm{ij}} \tag{3}$$

Where is the turbulent viscosity, k is the turbulent kinetic energy and δ_{ij} is the Kronecher delta function ($\delta_{ij} = 1$ if i=j and 0 if i≠j).

2.1.3. Turbulence model

The Shear-Stress Transport (SST) $k-\omega$ turbulence model has been used as it seems to be the most suitable to well-capture the essence of the relevant flow characteristics. Indeed several numerical studies based on finite volume method for Reynolds numbers in the subcritical range have recommended the use of SST $k-\omega$ model.
A recent study (Unal *et al.*, 2010) evaluates four Reynolds-Average Navier-Stokes (RANS) - based turbulence models in order to compare their accuracy in predicting some important flow field characteristics. The Spalart-Allmaras (S-A), the Realizable $k-\varepsilon$, the Wilcox $k-\omega$ and the SST $k-\omega$ turbulence models were investigated for a flow past circular cylinder at $\mathrm{Re} = 4.13\times10^4$. It derives that the SST k-ω model provides better results than the other one. Further 2D numerical study such as Mahbubar *et al*. (2007) investigated the wake behind a cylinder at Re= 3,900 using different turbulent models, the same observation has been made about the use of the SST $k-\omega$ model.

The turbulent kinetic energy k and dissipation kinetic rate ω equations for an incompressible flow are given by (FLUENT, 2005):

$$\rho \frac{\partial k}{\partial t} + \rho u_i \frac{\partial k}{\partial x_i} = \frac{\partial}{\partial x_j}\left(\Gamma_k \frac{\partial k}{\partial x_j}\right) + G_k - Y_k \tag{4}$$

$$\rho\frac{\partial\omega}{\partial t}+\rho u_i\frac{\partial\omega}{\partial x_i}=\frac{\partial}{\partial x_j}\left(\Gamma_\omega\frac{\partial\omega}{\partial x_j}\right)+G_\omega-Y_\omega+D_\omega \tag{5}$$

Where Γ_k and Γ_ω are respectively the effective diffusivity for k and ω. G_k and G_ω are respectively the generation of turbulence kinetic energy due to mean velocity gradients and the generation of ω. D_ω represents the cross-diffusion term.

2.2. Geometry

To solve the problem numerically, it is necessary to delimit the fluid domain. However some aspects concerning the dimensions of the physical domain have to be taken into account. Indeed the cylinder must be sufficiently distant from the inlet to not disturb the upstream incoming flow. Similarly the lateral boundaries must be far enough to the cylinder to not interfere with the cylinder wake. Moreover the distance between the cylinder and the outlet must be sufficient to allow wake visualization. To fulfil these previous remarks the 2D computational domain consists of an upstream length of *7d*, a downstream length of *17d* and a half width of *7d* from the cylinder centre as depicted in Fig. 1.

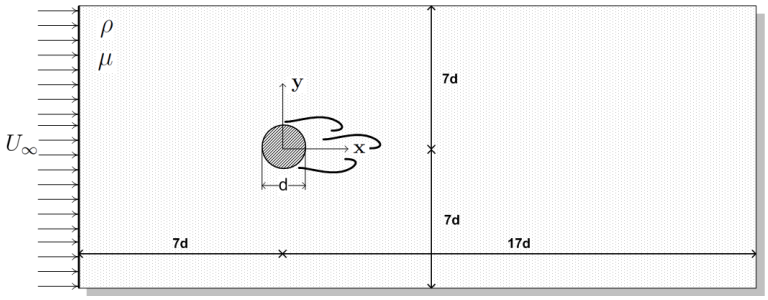

Figure 1. Problem description

2.3. Boundary conditions

Figure 2 summarizes the boundary conditions applied to the domain. GAMBIT software was used to generate the computational domain, mesh and determination of boundary conditions, as was used in other works (Honzejk and Fran, 2008). The inlet boundary condition is specified as velocity, with a constant profile normal to the boundary and so to the cylinder axis. The magnitude of the free-stream velocity U_∞ is set to 12m/s which leads to a Reynolds number around Re= 2,05 x 10^4 based on the cylinder diameter. The no-slip condition is imposed to the cylinder contour. The lateral boundaries are considered as translational periodic boundaries. Because of the cylinder is far enough to the lateral boundaries the flow in its vicinity is not considerably affected by the presence of the cylinder, the translational periodic boundaries allows to model the flow as if it was not confined. Finally the outlet boundary is defined as outflow.

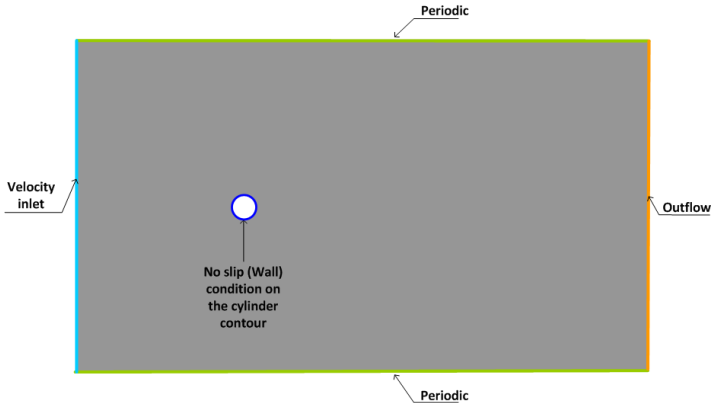

Figure 2. Boundary conditions applied to the domain

When using the SST $k-\omega$ turbulence model with an inlet velocity boundary condition additional parameters are required such as the turbulence kinetic energy k and the specific dissipation ratio ω. The following expressions are taken from Mahbubar *et al.* (2007).

The turbulence intensity I is determined using the following expression:

$$I = 0.16 Re^{-1/8} \tag{6}$$

The turbulence length scale l is defined as:

$$l = 0.007 d \tag{7}$$

The turbulent kinetic energy k can be obtained from the following relationship:

$$k = \frac{3}{2}(UI)^2 \tag{8}$$

Where U is the mean velocity.

Finally the specific dissipation ratio ω is expressed as follows:

$$\omega = C_{\mu}^{-1/4} \frac{\sqrt{k}}{l} \tag{9}$$

where $C_{\mu} \approx 0.09$ is an empirical value.

Table 1 summarizes the inlet velocity specifications for the present configuration.

Table 1. Specified values for the inlet velocity.

Present configuration	
Cylinder diameter	$0.025m$
Mean velocity	$12m/s$
Reynolds number	$20{,}538$
Results	
Turbulence intensity	4.6%
Turbulence length	$1.75\times10^{-3}m$
Turbulence kinetic energy	$0.46m^2/s^2$
Specific dissipation ratio	$709s^{-1}$

2.4. Grid and grid convergence study

Due to the simple geometry of a circular cylinder, the multi-block approach in the geometric modelling of the domain has been applied. It consists in decomposing the computational domain into sub-blocks with simple topologies and to generate structured grids within each sub-block. Several decompositions of the domain in simple topologies are possible. In the present study the domain is divided into ten blocks as shown in Fig. 3.

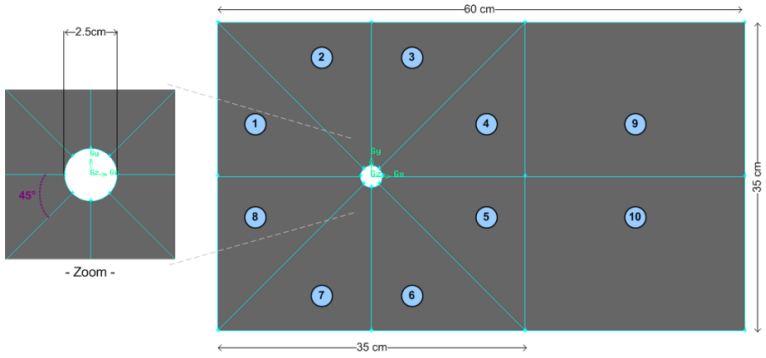

Figure 3. Decomposition of the domain into simple topologie

Each sub-block is discretized in a structured manner using a typical 2D quadrilateral element. An example of meshed domain is presented in Fig. 4.

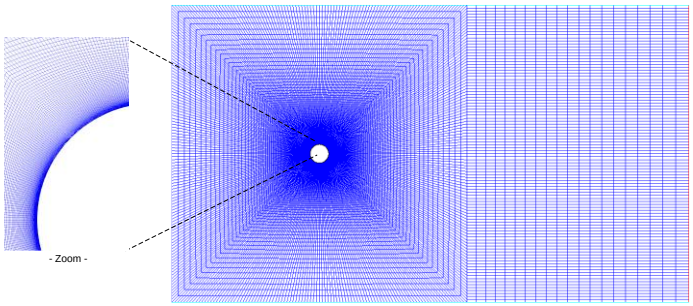

Figure 4. Example of meshed domain.

To emphasize the independence of the numerical solution regarding the grid resolution a set of meshes are investigated. The flow chart of the convergence study is given in Fig. 6. The monitored parameters are the mean drag , the r.m.s lift coefficient $C_{L'}$, the Strouhal number S_t and an additional parameter representing the maximum angular deviation of the grid Q_{EAS} to track down the grid quality. However due to the large amount of simulation time necessary to complete this study, a converged solution has not yet been to reach. The comparison of the results obtained from the different meshes already investigated are given in Tab. 2 and depicted in Fig. 5.

Table 2. Grid convergence results.

Mesh		Cylinder nodes	Nodes normal to cyl.	Total nodes			
M1	0.5	400	100	44440	0.91	0.15	0.21
M2	0.5	640	160	109480	1.01	0.33	0.21
M3	0.5	720	180	137560	1.05	0.40	0.20
M4	0.5	880	220	203320	1.09	0.50	0.17

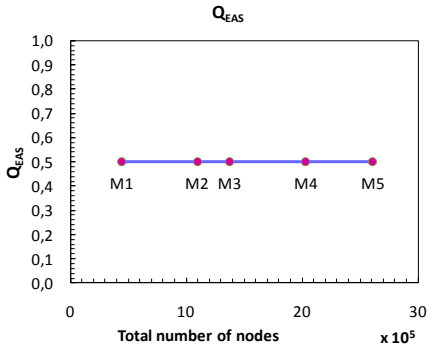

a) Equi Angle Skew Q_{EAS} convergence

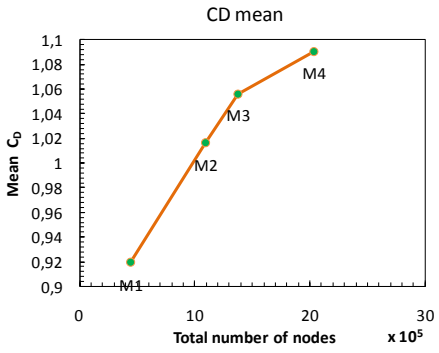

b) Mean drag coefficient convergence

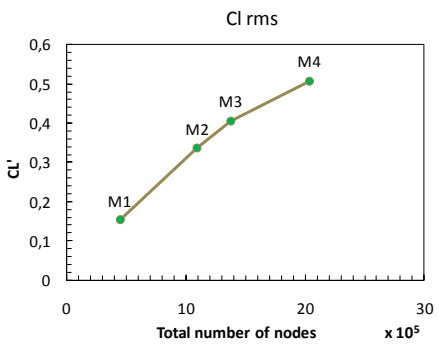

c) R.m.s lift convergence

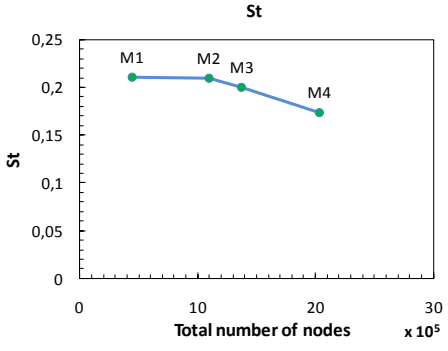

d) Strouhal number convergence

Figure 5. Results of the convergence study.

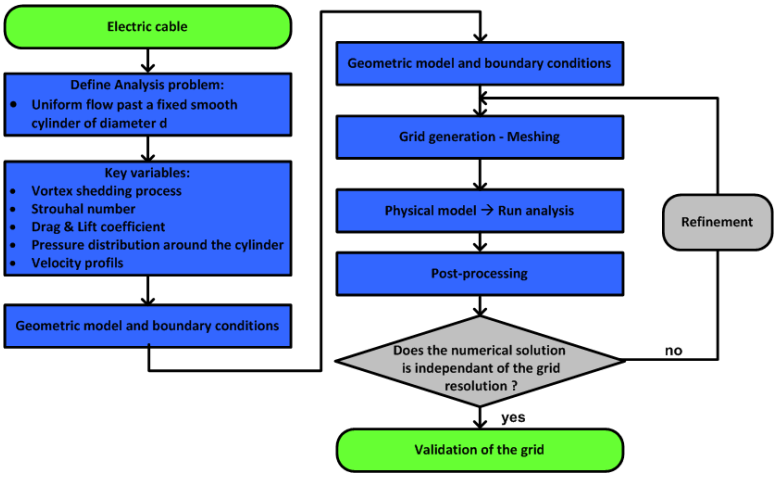

Figure 6. Flowchart of the convergence study

2.5. Summary - Simulation Settings

The simulations were performed using a computer with an Intel Core 2 Duo CPU and 2 GB of RAM. The fluid properties as density and viscosity have been taken from the software material property database. The simulation settings and other important parameters of the last investigated mesh are given in Tab. 3.

The PISO scheme is one of the four algorithms present in FLUENT responsible for meeting the requirement of pressure - velocity coupling and is recommended for all calculations of transient flow and was used in the simulation because it offers better efficiency calculation since this algorithm works with two patches additional which consider more iterations to satisfy the continuity and momentum equations and calculation conditions for meshes with some degree of asymmetry.

Table 3. 2D simulation for mesh M4

Settings	
Simulation	2D finite volume
Fluid Density Dynamic viscosity	Air - Newtonian, incompressible $\rho_{air} = 1.225 kg/m^3$ $\mu_{air} = 1.7894 \times 10^{-5} kg/(m.s)$
Boundary conditions	Inlet: inlet velocity Outlet: outflow Lateral: periodic Cylinder contour: wall (no-slip)
Solver Unsteady formulation Turbulence model Pressure Pressure-velocity coupling Momentum, k and ϵ equations Iteration	Segregated implicit, unsteady 2nd order implicit SST k-ω Standard discretization PISO 2nd order upwind discretization Time step size: $4 \times 10^{-4} s$ Fixed time step option Max. iteration per time step: 20
Distance cylinder – 1st grid point Element types Total number of nodes Grid quality -	$0.45\% d = 1.125 \times 10^{-5} m$ Quad Map 203320 *0.5*

3. RESULTS AND DISCUSSION

As mentioned previously a converged solution has not yet been reached, nevertheless the simulation exhibits the physical characteristics of the flow past a smooth cylinder and are presented bellow. This part presents the obtained results for mesh M4.

3.1. Vortex shedding phenomenon

Figure 7 presents the developing stages within a vortex shedding cycle. It can be seen that the flow around a fixed circular cylinder generates an instable velocity profile in its wake. Vortices are shed alternatively from the upper and lower surfaces of the cylinder creating a periodic flow pattern known as the Kármán vortex street.

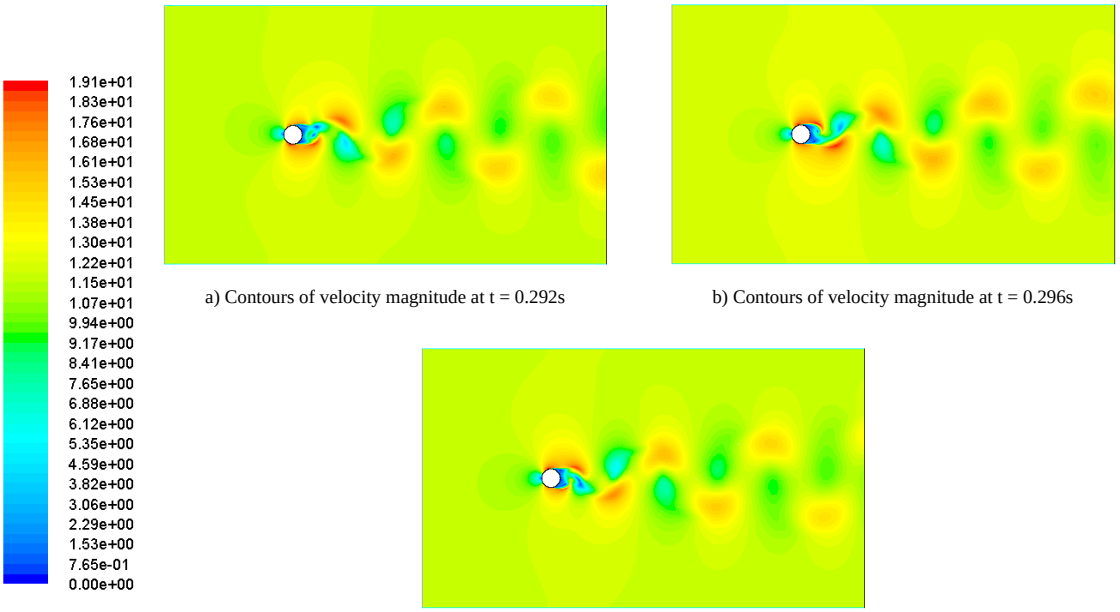

a) Contours of velocity magnitude at t = 0.292s

b) Contours of velocity magnitude at t = 0.296s

c) Contours of velocity magnitude at t = 0.3s

Figure 7. Developing stages within a vortex shedding cycle

The vortex shedding frequency f_s varies proportionally to the flow velocity and inversely to the cylinder diameter:

$$f_s = S_t \frac{U}{d} \tag{10}$$

Where U is the flow velocity, d is the cylinder diameter and S_t is the Strouhal number.

Figure 8a. corresponds to spectrum analysis of the lift coefficient time history using the Power Spectral Density (PSD) method. It can be seen that the spectral band is narrowed and sharpened with a well-defined frequency of approximately $80Hz$. This traduces that the phenomena of vortex shedding occurs in a regular and well-defined manner. (Norberg, 2003) recapitulates a number of experiments related to the Strouhal number as shown in Fig. 8-b. The Strouhal number obtained from simulation is compared with the previous experimental results.

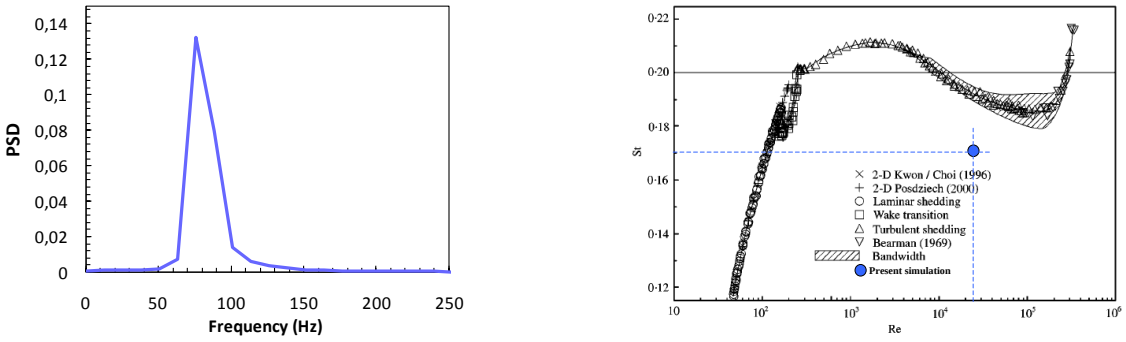

a) PSD of the time history lift C_L.

b) S_t Vs. Re. From (Norberg, 2003).

Figure 8. Shedding frequency and Strouhal number.

3.2. Lift and drag coefficients

Due to the vortex shedding, both the drag and lift coefficients oscillate as shown in Fig. 9. The mean drag coefficient $\overline{C_D}$ is 1.1 while the mean lift $\overline{C_L}$ can be considered as zero. The peak to peak values for respectively the lift and drag coefficients are $\Delta C_L = 1.43$ and $\Delta C_D = 0.16$. The frequency of the fluctuating lift and drag are closely related to the shedding frequency f_s. The lift fluctuates periodically at the frequency f_s while the drag at twice f_s. These can be interpreted physically as follows: the sign of the lift depends on the location of the vortex i.e. above (+) and bellow (-) the cylinder. Besides, the lift reaches one maximum and one minimum respectively when a vortex is shedded from the upper part and the lower part of the cylinder. During the process of growth and shedding the drag has one maximum and one minimum. When the phenomenon is stabilized the lift can be modelled by the following equation (Norberg, 2003):

$$C_L = \sqrt{2} C_{L'} \sin(f_s t) \tag{11}$$

A suggested formulation for drag coefficient, , can be given as follows:

$$C_D = \overline{C}_D + 1/2 \Delta C_D \sin(2 f_s t) \tag{12}$$

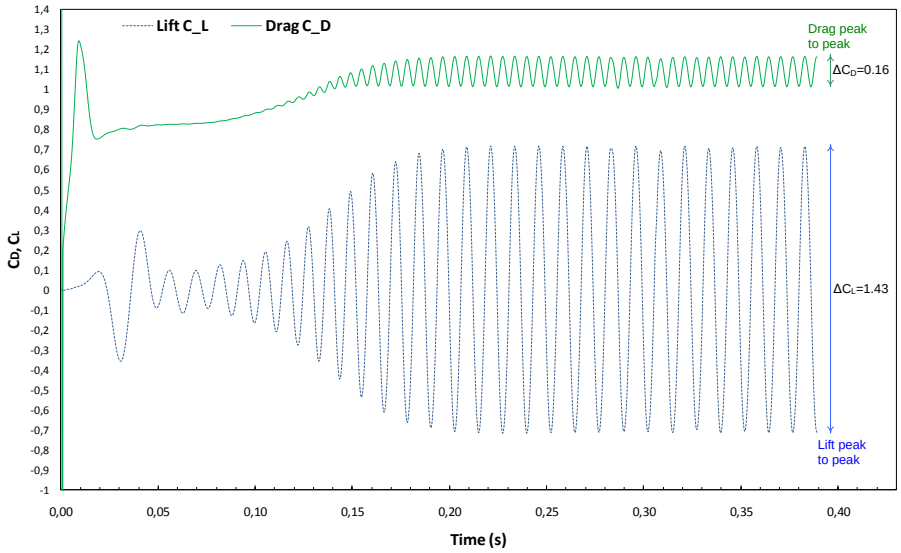

Figure 9. Temporal variations of the lift and the drag coefficients.

Norberg (2003) also provides a set of r.m.s. lift coefficient $C_{L'}$ for different regions by considering values from many experiments as shown in Fig. 10. The obtained r.m.s lift for mesh *M4* is in good accordance these results.

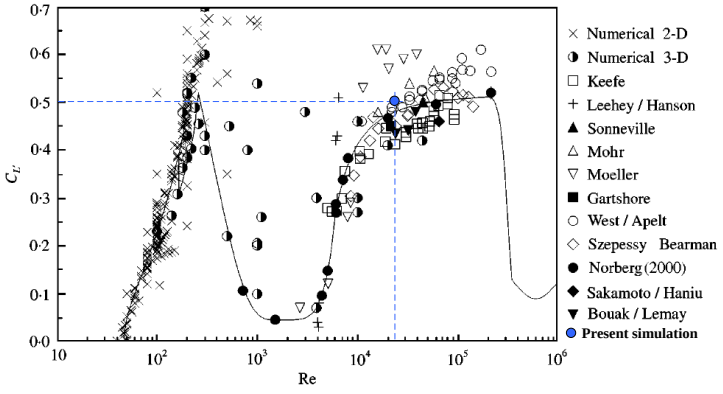

Figure 10. vs. Re. In solid line the empirical formulation. From (Norberg, 2003).

The mean drag coefficient also complies with literature as shown in Fig. 11.

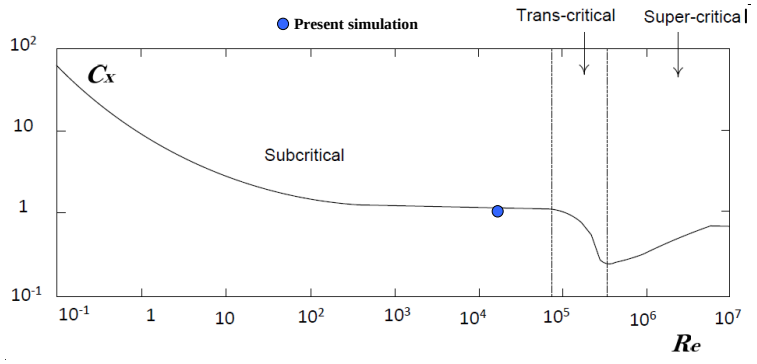

Figure 11. vs. Re. Adapted from (Hémon, 2006)

4. CONCLUSION

This study in its beginning seeks to illustrate such an endeavour by understanding the effect of the wind on an electric cable. In this first approach the conductor was modelled as a smooth fixed circular cylinder. The 2D simulation has been performed using the SST $k-\omega$ turbulence model. The computational domain and mesh were generated using the software GAMBIT and through the variation of the number of elements in the discretization of the domain, it was possible to conduct a study of mesh and check which one offered the best results. Unfortunately since the convergence study has not yet been completely fulfilled, some more refinements have to be made. Nevertheless some important aspects can already be appreciated. The flow around the fixed cylinder generates an instable velocity profile in its wake. Vortices are shed alternatively from the upper and lower surfaces of the cylinder creating a spatial and temporal periodic flow pattern known as the Von - Kármán Vortex Street. Consequence upon the difference of flow velocity between the inner and outer part of the wake leads to the development of vortices.
When the model shall be validated some further investigations could be carried out in order to capture in a more realistic manner the phenomenon of wind-induced vibrations that lead to important lifetime matters due to the fatigue undergoes by the conductor.

5. REFERENCES

FLUENT Inc. FLUENT 6.2.16, User's guide volume. Lebanon, 2005

Hémon, P., 2006, "Vibrations Couplées avec le Vent", ISBN: 2-7302-1332-5

Honzejk, V., Fraña, K., 2008, " A Turbulent Flow Past a Cylinder", Journal of Applied Science in the Themodynamics and Fluid Mechanics, vol 2, nº 2.

Leonard, A., Roshko, A. , 2001, "Aspects of Flow - Induced Vibration", Journal of Fluids and Structures 15, pp. 415-425.

Mahbubar, R., Mashud, K., and Abdul, A., 2007, "Numerical Investigation of Unsteady Flow past a Circular Cylinder Using 2-D Finite Volume Method", Journal of Naval Architecture and Marine Engineering.

Norberg, C, 2003, "Fluctuating Lift on a Circular Cylinder: Review and New Measurements", Journal of Fluids and Structures 17 (1), pp. 57-96.

Sumer, B.M., Fredsoe, J., 2006, "Hydrodynamics around Cylindrical Structures - Revised Edition", World Scientific - Advanced Series on Ocean Engineering - Volume 26.

Unal, U.O., Atlar, M., and Gören O., 2010, "Effect of Turbulence Modeling on the Computation of the Near-Wake Flow of a Circular Cylinder", Ocean Engineering 37, pp. 387-399.

Williamson, C.H.K., 1996, "Vortex Dynamics in the Cylinder Wake", Annual Review of Fluid Mechanics 28, pp. 477-539.

6. RESPONSIBILITY NOTICE

The authors are the only responsible for the printed material included in this paper.